In-situ Lorentz TEM Cooling Study of Magnetic Domain Configurations in Ni_2MnGa

Marc De Graef, Matthew A. Willard, Michael E. McHenry, and Yimei Zhu

***Abstract*—Magnetic domain configurations in the ferromagnetic shape memory alloy Ni_2MnGa are analyzed by means of Lorentz microscopy and noninterferometric phase reconstruction methods. Domain structures in the cubic phase consist of cross-tie walls in the thinnest portions of the foil, and more complex configurations in thicker regions. At low temperature, the magnetization configurations change as the structure transforms martensitically to a tetragonal phase. A simple model for the magnetization changes is proposed.**

***Index Terms*—Ferromagnetic shape memory alloy, magnetic domains, phase reconstruction, phase transformation.**

I. Introduction

THE FERROMAGNETIC shape memory alloy Ni_2MnGa has been the subject of intensive investigations during the last decade. The alloy has the potential to provide a magnetically driven shape memory effect, with a total reversible shape change (linear strain) of about 6% [1]. The ferromagnetic cubic phase has the Heusler $L2_1$ structure with $a = 0.588$ nm [2], and the easy axes are of the $\langle 111 \rangle$ type. The low temperature phase is tetragonal with $a = 0.59$ nm and $c = 0.544$ nm for the stoichiometric composition. The $[001]$ direction is the easy axis below the martensitic transformation temperature, and there are 3 possible orientations of the tetragonal phase with respect to the cubic parent phase. Despite significant interest in the magnetic properties of this intermetallic, no systematic studies of the magnetic domain structure have been carried out to date.

The close correlation between crystallographic twins and magnetic domain walls in the martensitic state raises questions about their mutual interactions: Do twin boundaries and magnetic domain walls coincide? What is the relation, if any, between the magnetic domain wall width and the twin boundary thickness [3]? Are the pinning centers for the magnetic domain walls the same as those for the crystallographic twins? How does the magnetization direction change during the cubic-to-tetragonal martensitic transformation (a theoretical phase diagram proposed by Vasilev [4] suggests the existence of a canted ferromagnetic phase in a temperature range near the martensitic transformation temperature)? Each of these questions requires a careful characterization of magnetic domain configurations and crystallography of the twin variants.

In this paper we report on the first Lorentz microscopy observations of the magnetic domain structure in the stoichiometric compound Ni_2MnGa, using *in-situ* cooling through the martensitic transformation temperature. The Lorentz images are analyzed using a recently developed noninterferometric phase reconstruction technique [5], [6], and first we briefly review the theory. Then we present experimental observations of the changes in the domain wall configurations during the martensitic transformation and introduce a simple model.

II. Experimental Methods

Lorentz microscopy observations were carried out in a JEOL 3000F field emission TEM at Brookhaven National Laboratory, using a Gatan liquid nitrogen double tilt cooling stage. The microscope was operated in free lens control mode at 300 kV with the main objective lens turned off. Images were acquired through a Gatan Imaging Filter (GIF), operated in zero loss mode with a 20 eV energy selecting slit. Additional room temperature observations were carried out in a JEOL 4000EX, operated at 400 kV with the main objective lens turned off; again a GIF was used to acquire the images.

Lorentz images in Fresnel imaging mode can be analyzed quantitatively using the Paganin&Nugent phase reconstruction method [5]. The method relies on the so-called *Transport-of-Intensity Equation* or TIE [7], which relates the intensity variation $\partial_z I$ along the propagation direction to the variation of the phase ϕ of the wave in a plane normal to the propagation direction:

$$\nabla_\perp \cdot (I(\mathbf{r}_\perp)\nabla_\perp \phi(\mathbf{r}_\perp)) = -k\partial_z I(\mathbf{r}_\perp), \tag{1}$$

with $\mathbf{r}_\perp$ a vector in the image plane, $k = 2\pi/\lambda$ the relativistic wavenumber, and $\nabla_\perp$ the two-dimensional gradient operator. A formal solution to this equation was proposed in [5] and further simplified in [8]:

$$\phi(\mathbf{r}_\perp) = \frac{\delta^2}{2\pi\lambda\Delta f} \sum_{i=1}^{2} \rho_i \otimes \left[\frac{\rho_i \otimes \partial_z I(\mathbf{r}_\perp)}{I(\mathbf{r}_\perp)} \right], \tag{2}$$

where

- $\otimes$ denotes the convolution product,
- δ the image pixel size (in nm per pixel), and
- Δf the microscope defocus used to obtain the derivative $\partial_z I$.

Manuscript received October 3, 2000.

This work was supported in part by the National Science Foundation under CAREER Grant DMR 95-01017, and the Department of Energy under Contract DE-AC02-98CD10886.

M. De Graef and M. E. McHenry are with the Department of Materials Science and Engineering, Carnegie Mellon University, Pittsburgh, PA, USA (e-mail: degraef@cmu.edu; mm7g@andrew.cmu.edu).

M. A. Willard is with the Naval Research Laboratory, Washington DC, USA (e-mail: willard@anvil.nrl.navy.mil).

Y. Zhu is with the Materials Science Division of Brookhaven National Laboratory, Upton, NY, USA (e-mail: zhu@bnl.gov).

Publisher Item Identifier S 0018-9464(01)07203-X.

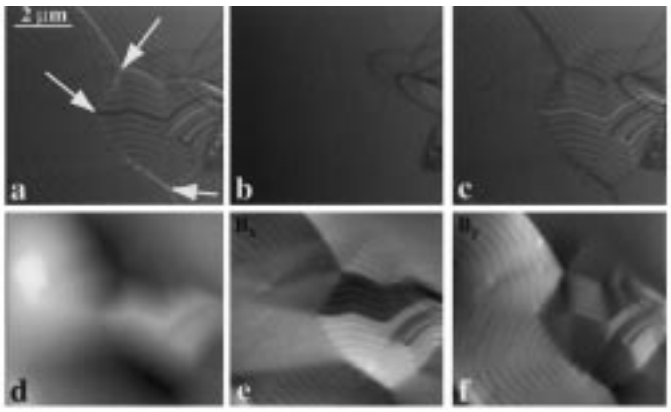

Fig. 1. (a)–(c): Through-focus series (room temperature, 400 kV) of thicker region of thin foil of Ni_2MnGa, oriented close to $[001]$, (d) is the reconstructed phase ϕ, and the magnetic induction components B_x and B_y, the components of the gradient of ϕ, are shown in (e) and (f).

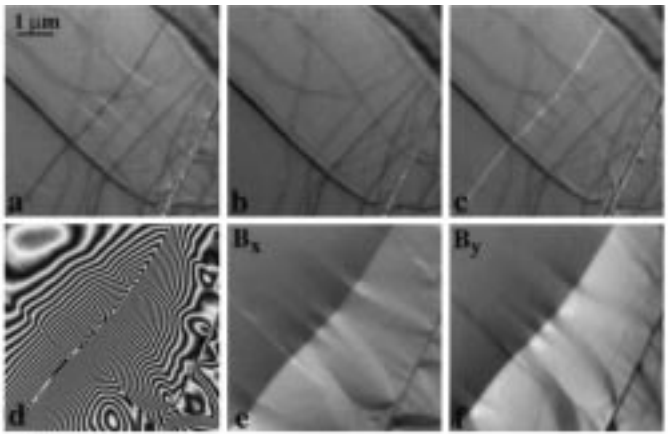

Fig. 2. Same set of images as in Fig. 1, recorded in the thinner section of the foil. A 180° domain wall runs from lower left to upper right, and has several cross-tie walls along its length. The phase map (d) shows $\cos\phi$.

The vector components ρ_i are defined by

$$\rho_x \mathbf{e}_x + \rho_y \mathbf{e}_y = \mathcal{F}^{-1}\left[\frac{\mathbf{q}_\perp}{|\mathbf{q}_\perp|^2}\right],$$

with $\mathcal{F}$ the Fourier transform operator, and $\mathbf{q}_\perp$ the in-plane spatial frequency vector. The entire procedure can be implemented efficiently using 4 fast Fourier transforms. The input parameters are 3 images (under-, in-, and over-focus), and the calibrated values for λ, δ and Δf. The phase reconstruction takes less than 1 second for a 512×512 image on a 666 MHz Compaq TRU64 UNIX workstation.

III. Observations and Discussion

A $[001]$-oriented thin foil was obtained from the same Ni_2MnGa boule as that used for the neutron diffraction experiments reported in [9]. The foil was mounted in the double tilt cooling holder in a JEOL 3000F and cooled down to 116 K. Strong tweed contrast was observed between room temperature and the onset of the martensitic transformation at around 220 K. Due to the large transformation strain, no images could be obtained during the martensitic transformation, as the lateral sample movement was significant. The typical magnetic domain configuration at room temperature consisted of long 180° domain walls with arrays of 71° domain walls in between. Fig. 1(a)–(c) shows a through focus series [(a) = under-focus, (b) = in-focus, (c) = over-focus, obtained at 400 kV] of a set of 180° walls [bright line near top and dark line near center in Fig. 1(a)], which split into 90° walls at the arrowed locations. The striations in parallel to the 180° walls are caused by 71° domain walls, with an average spacing of about 300 nm. The character of these walls can be inferred from the phase reconstructed magnetization maps. Fig. 1(c) shows a gray-scale phase map; ridges and valleys correspond to the 180° domain walls. The gradient of the phase results in the B_x and B_y magnetization components (multiplied by the local sample thickness), and are shown in Fig. 1(e) and (f), respectively. The easy magnetization axes are of the $\langle 111 \rangle$ type, and all these directions have an out-of-plane component for a $[001]$ oriented foil. The striated pattern of 71° walls (the angle between two $\langle 111 \rangle$ directions in a cubic system) arises through a minimization of the demagnetization field, which makes the magnetization vectors alternate between a positive and a negative out-of-plane component. The largest in-plane induction then arises at the domain walls, where the Lorentz beam deflection is strongest. Lorentz image simulations on a model array of 71° agree with the main image features in Fig. 1.

In the thinnest portions of the foil, the domain wall patterns are significantly different from the striated patterns shown in Fig. 1. No striations are observed near the edge of the thin foil, and most 180° domain walls show arrays of cross-tie walls. An example cross-tie wall is shown in Fig. 2: the top row shows a through-focus series with the 180° wall running from lower left to upper right. Fig. 2(d) shows the reconstructed phase ($\cos\phi$) and the magnetization components are shown in (e) and (f). The vortices are clearly visible as nearly circular phase contours in Fig. 2(d).

Fig. 3 shows a diamond-shaped domain wall feature that is often observed in the cubic phase (room temperature, 400 kV). Fig. 3(a)–(c) again represent the under-focus, in-focus, and over-focus images, respectively. The reconstructed phase is shown as $\cos\phi$ in (d), and as a shaded surface in (g). The magnetization configuration derived from the phase is shown in Fig. 3(e) and (f). From the reconstructed magnetization one can derive a schematic representation of the magnetization profile, shown in (h). This can in turn be used to compute the phase of the electron wave, using the Mansuripur algorithm [10]; the resulting theoretical phase profile is shown in Fig. 3(i). The qualitative agreement between the measured and the theoretical phase profiles is remarkably good. The theoretical phase can then be used to compute Fresnel (out-of-focus) images, which are shown as insets in Fig. 3(a) and (c).

Fig. 4(a)–(c) shows a through-focus series of a fully transformed area of martensite plates (300 kV, 118 K). Two types of domain wall contrast can be observed: in the upper region of the micrograph, short domain wall segments are present between neighboring martensite plate boundaries. The segments occur at various orientation with respect to the twin boundaries, from nearly normal to nearly parallel. The lower portion of the micrograph shows domain walls which are parallel to the twin boundaries. This is more clearly observed in the reconstructed

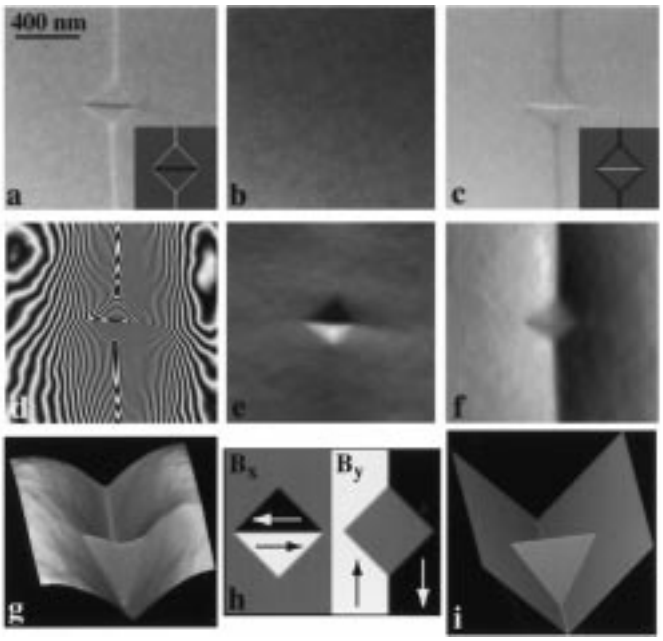

Fig. 3. Same set of images as in Fig. 1 for a diamond shaped domain wall feature in the thinner region of the foil. The phase map is shown as a shaded surface in (g). The magnetization schematic in (h) was used to compute the theoretical phase profile in (i), and the resulting out-of-focus images are shown as insets in (a) and (c).

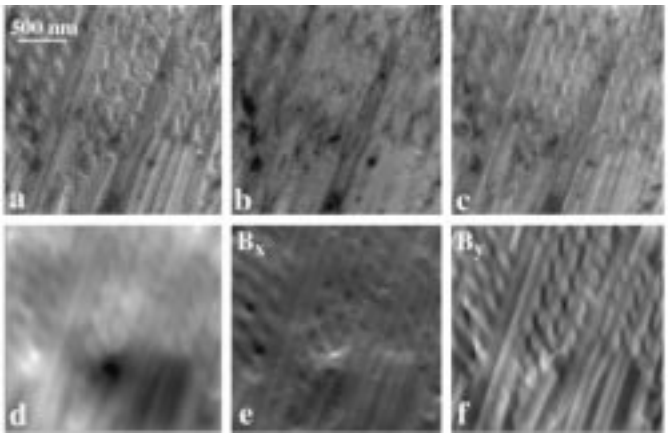

Fig. 4. Similar set of images as in Fig. 1, taken at 300 kV and 118 K. The martensite plates are clearly visible. Two different domain geometries are observed, as discussed in the text.

magnetization maps, Fig. 4(e) and (f), where the alternating contrast of the B_y-component indicates the presence of 180° domain walls along the twin boundaries. Fig. 4(d) is the corresponding reconstructed phase map. The different domain wall configurations in this micrograph indicate that the change of the easy axes from $\langle 111 \rangle$ in the cubic phase to $[001]$ in the tetragonal phase does not occur at the same time as the growth of the martensite plates. The alternating 71° domain walls shown in Fig. 1 are first intersected by the martensite plates. Subsequently, the now smaller domain segments rotate until the magnetization direction lies parallel to the twin planes.

IV. Conclusions

The magnetic domain structure in Ni_2MnGa was analyzed by means of Lorentz microscopy and noninterferometric phase reconstruction. In the cubic phase 180° domain walls are dominant, along with regular arrays of 71° walls with an average spacing of 300 nm. In the thinnest sections of the TEM foil cross-tie walls and diamond shaped configurations were observed. The observations indicate that there is a critical thickness below which the nature of the magnetic domains changes. This may be of importance for thin film actuator applications of these materials. At low temperature the magnetization rotates so that the domain walls coincide with the martensite twin boundaries. A more detailed study of this mechanism is currently underway.

Acknowledgment

The authors wish to acknowledge S. Volkov, L. Wu, and M. Schofield for stimulating discussions, and S. Shapiro and L.E. Tanner for providing the Ni_2MnGa single crystal thin foils.

References

[1] S. J. Murray, M. Farinelli, C. Kantner, J. K. Huang, S. M. Allen, and R. C. O'Handley, "Field-induced strain under load in Ni–Mn–Ga magnetic shape memory materials," *J. Appl. Phys.*, vol. 83, pp. 7297–7299, 1998.

[2] P. J. Webster, K. R. A. Ziebeck, S. L. Town, and M. S. Peak, "Magnetic order and phase transformation in Ni_2MnGa," *Philosophical Magazine B*, vol. 49, pp. 295–310, 1984.

[3] G. R. Barsch and J. A. Krumhansl, "Twin boundaries in ferroelastic media without interface dislocations," *Phys. Rev. Lett.*, vol. 53, p. 1069, 1984.

[4] A. N. Vasil'ev, A. D. Bozhko, V. V. Khovailo, I. E. Dikshtein, V. G. Shavrov, V. D. Buchelnikov, M. Matsumoto, S. Suzuki, T. Takagi, and J. Tani, "Structural and magnetic phase transitions in shape-memory alloys $Ni_{2+x}Mn_{1-x}Ga$," *Phys. Rev. B*, vol. 59, pp. 1113–1121, 1999.

[5] D. Paganin and K. A. Nugent, "Noninterferometric phase imaging with partially coherent light," *Phys. Rev. Lett.*, vol. 80, pp. 2586–2589, 1998.

[6] A. Barty, D. Paganin, and K. A. Nugent, "Phase retrieval in Lorentz microscopy," in *Magnetic Microscopy and its Applications to Magnetic Materials*, M. De Graef and Y. Zhu, Eds: Academic Press, 2000, vol. 36, Experimental Methods in the Physical Sciences.

[7] M. R. Teague, "Deterministic phase retrieval: A Green's function solution," *J. Opt. Soc. Am.*, vol. 72, pp. 1199–1209, 1982.

[8] M. De Graef and Y. Zhu, "Quantitative noninterferometric Lorentz microscopy," J. Appl. Phys., 2000, submitted for publication.

[9] A. Zheludev, S. M. Shapiro, P. Wochner, A. Schwartz, M. Wall, and L. E. Tanner, "Phonon anomaly, central peak, and microstructures in Ni_2MnGa," *Phys. Rev. B*, vol. 51, pp. 11 310–11 314, 1995.

[10] M. Mansuripur, "Computation of electron diffraction patterns in Lorentz electron microscopy of thin magnetic films," *J. Appl. Phys.*, vol. 69, pp. 2455–2464, 1991.

[11] S. Bajt, A. Barty, K. A. Nugent, M. McCartney, M. Wall, and D. Paganin, "Quantitative phase-sensitive imaging in a transmission electron microscope," *Ultramicroscopy*, vol. 83, pp. 67–74, 2000.